Interpretation of the magnetotelluric impedance tensor: regional induction and local telluric distortion

Karsten Bahr*

Ocean Research Division A-030, Scripps Institution of Oceanography, UCSD, La Jolla, Ca. 92093, U.S.A.

Abstract. A method for the interpretation of the magnetotelluric (MT) impedance tensor, the telluric-vector technique, is presented. The phase information of all impedance tensor elements is used to distinguish between local telluric distortion and regional induction. A model incorporating a superposition of the effects of local surface anomalies and a regional 1-D, 2-D or 3-D conductivity distribution is applied. In 2-D regional structures, a complete separation of the contributions of local and regional anomalies is possible if additional information from geomagnetic depth sounding (GDS) is used. A new skewness parameter derived from phases alone is introduced to measure the three-dimensionality of the regional structure independent of local distortions.

Key words: MT tensor — Static shift — Structural dimensionality — Separation into local and regional contributions

Introduction

Recently, two problems have often hindered an accurate interpretation of the magnetotelluric impedance tensor: (1) static shifts and (2) the so-called 'three-dimensionality' of the tensor. The first is caused either by local zones of anomalous conductivity, which are small compared to the penetration depth, or by folding of the stratum. These change the electric field in direction and magnitude. Thus, instead of an impedance, which correctly describes the resistivity of the subsoil, a 'shifted' impedance is obtained. The second problem paraphrases the fact that there is no coordinate system in which the diagonal elements of the impedance tensor disappear. Therefore, a model with a three-dimensional conductivity distribution must be used to explain the tensor impedance at a single site.

These two difficulties are of course somewhat related but have almost always been handled separately. Some authors remove a frequency-independent distortion matrix (Larsen, 1977; Kemmerle, 1977) and extract a scalar impedance from the remaining tensor. Others do not deal with the distortion matrix, but rather examine the inner properties of the impedance tensor. Both Swift's (1967) diagonal minimization method for finding the strike in a 2-D structure as well as his use of the 'skewness' coefficient as a

* *Present address:* Institut für Geophysik der Universität Göttingen, Postfach 2341, D-3400 Göttingen, Federal Republic of Germany

measure of deviation from two-dimensionality have been widely applied. In the pure 2-D case the electromagnetic field is split into two separate modes, in each of which the electric and magnetic fields are perpendicular. Therefore, the diagonal elements of the impedance tensor should vanish as it is expressed by Swift's condition. More recently, some authors forsook the demand for orthogonal electric and magnetic fields. Eggers' (1982) eigenstate analysis of the impedance tensor allows for other angles between the two fields. He and some subsequent authors (La Torraca et al., 1986; Cevallos, 1986) suggest a more mathematical decomposition of the impedance tensor that retains all the information contained in the four complex impedances. However, these papers give no proof of the physical significance of the parameters extracted from the impedance tensor. Counil et al. (1986) also deal with non-orthogonal electric and magnetic bases. A detailed comparison of these decomposition methods is given by Yee and Paulson (1987).

In this paper the MT impedance tensor will be explained by a superposition of regional and local conductivity anomalies. 'Regional' means that the horizontal dimensions are comparable with the depth of penetration. 'Local' structures are much smaller than the penetration depth: they cause DC distortion. It will be shown that the conventional analysis, using orthogonal electric and magnetic bases, sufficiently describes a regional 2-D anomaly if the contribution of the local structure has been removed from the tensor. A new 'skewness' coefficient, that takes into account the three-dimensionality of the regional conductivity distribution only, will be introduced.

Regional 1-D resistivity distribution and local 3-D distortion

In magnetotellurics one assumes that in the frequency domain the horizontal electric field **E** and the horizontal magnetic field **B** are linked through the impedance tensor **Z**:

$$\mathbf{E} = \mathbf{Z} \cdot \mathbf{B}.$$

For a resistivity distribution which is purely depth dependent except for a thin top layer of varying conductance, the general impedance tensor

$$\mathbf{Z} = \begin{pmatrix} a_{11} & a_{12} \\ a_{21} & a_{22} \end{pmatrix} \begin{pmatrix} 0 & Z_n \\ -Z_n & 0 \end{pmatrix} \tag{1}$$

will be obtained. The normal impedance Z_n contains all the depth sounding information. The distortion matrix ele-

ments a_{11}, a_{12}, a_{21}, a_{22} are independent of frequency and real in the frequency range in which the penetration depth is large compared to the extension of the top layer structures. All elements of a measured impedance tensor must have the same phase if they are to be described by Eq. (1). They yield four real values which are multiples of the elements of the distortion matrix and the phase factor of the normal impedance Z_n. A sixth degree of freedom is required to obtain the true magnitude of Z_n. So far, this distortion factor has been found by two methods:

1) Additional information about the top layer: Kemmerle (1977) pursued conductivity contrasts in the top layer with geoelectric methods in order to determine the elements of the distortion matrix.

2) Additional information about the mantle conductivity: Larsen (1977) calculated an undistorted impedance from the ratio of the vertical to the horizontal component of the Sq variation field. This '$Z:H$ method' was originally set up by Eckhardt (1963). Schmucker (1974) applied it to Sq variations. By expanding the frequency range of the MT method up to daily variations, the MT impedance can be linked to the undistorted impedance found with the $Z:H$ method. The resulting distortion matrix can be applied to all shorter periods as long as only one phase appears in the impedance tensor. If this is the case, Eq. (1) is a valid model and the regional conductivity distribution can be considered 1-D.

Regional 2-D resistivity distribution and local 3-D distortion

The superposition of a large-scale regional 2-D conductivity anomaly and local resistivity changes in the top layer yields the general impedance tensor

$$Z = A \cdot \begin{pmatrix} 0 & Z'_{xy} \\ -Z'_{yx} & 0 \end{pmatrix}, \tag{2}$$

usually with different amplitudes and phases in Z'_{xy} and Z'_{yx}. Here, as well as in the subsequent sections, cartesian coordinates (x, y) refer to observations while coordinates (x', y') refer to a regional 2-D structure with x' normal to strike. The prime (') indicates tensor elements in coordinates (x', y'), i.e. Z'_{xy} means $Z_{x'y'}$ for shortness. A is the distortion matrix. In using Eq. (2) we postulate that the appropriate coordinate system has already been found. This topic will be pursued in a later section. Additional information is necessary to obtain the correct amplitudes of the two impedances Z'_{xy} and Z'_{yx}. Apart from the impedance splitting according to Eq. (2), the large-scale regional anomaly causes a regional amplification of the vertical magnetic component B_z as well as spatial changes of the horizontal magnetic components B_x and B_y. With the 'geomagnetic depth sounding' method these changes can be deduced from simultaneous magnetic recordings at different sites. They can be used as an additional help for modelling the regional conductivity anomaly. The spatial differences between the magnetic fields at two sites (1, 2) are usually presented, following a suggestion by Schmucker (1970), by a perturbation matrix:

$$\begin{pmatrix} B_x(1) - B_x(2) \\ B_y(1) - B_y(2) \\ B_z(1) - B_z(2) \end{pmatrix} = \begin{pmatrix} h_H & h_D \\ d_H & d_D \\ z_H & z_D \end{pmatrix} \begin{pmatrix} B_x(2) \\ B_y(2) \end{pmatrix}. \tag{3}$$

The six complex dimensionless transfer functions $h_H, \ldots, z_D$ describe a linear relation between the components of the magnetic fields at two sites. If the conductivity varies only in one horizontal direction as described by Eq. (2), all elements except h_H and z_H in a suitable coordinate system will vanish. h_H and z_H belong to the E-polarization.

The 'conductivity reference' method

This section deals with situations where the strike of a regional structure, taken to be 2-D, is known from geology.

The combination of magnetotellurics and geomagnetic depth sounding (Bahr, 1983; Cerv et al., 1984) offers a powerful tool in overcoming the handicap that the impedances Z'_{xy} and Z'_{yx} in Eq. (2) are unknown. This is demonstrated with the interpretation of field data from station LAU (Laubach) in the Rhenish Massif, an uplifted and exposed section of the Variscian mountain belt in central Europe (see Fig. 1). The SW-NE-striking Hunsrück south edge, the so-called "Hunsrück-Südrandverwerfung" as a deep-reaching tectonic lineament between highly resistive Variscian sediments of the Rhenish Massif and unfolded past-Variscian sediments of higher conductivity, is described by a 2-D model. Three sets of field data are interpreted:

1) The tensor impedance, free from local distortions, of the 'reference station' SPO (Sponsheim) situated at the lower part of the Nahe river.

2) The tensor impedance at LAU in coordinates (x', y') rotated anti-clockwise by 40°. Z'_{yx} is the impedance of E-polarization and Z'_{xy} is the impedance of B-polarization.
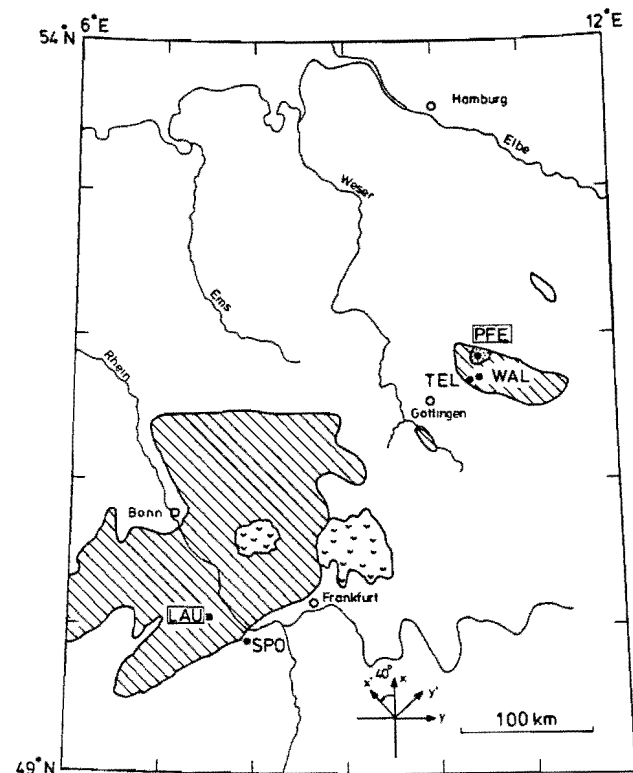

Fig. 1. MT sites within the Rhenish Massif and Harz Mountains (hatched areas) of the uplifted and exposed Variscian mountain belt in West Germany. (v) Tertiary volcanic areas of Vogelsberg and Westerwald, (···) gabbro massif of Bad Harzburg
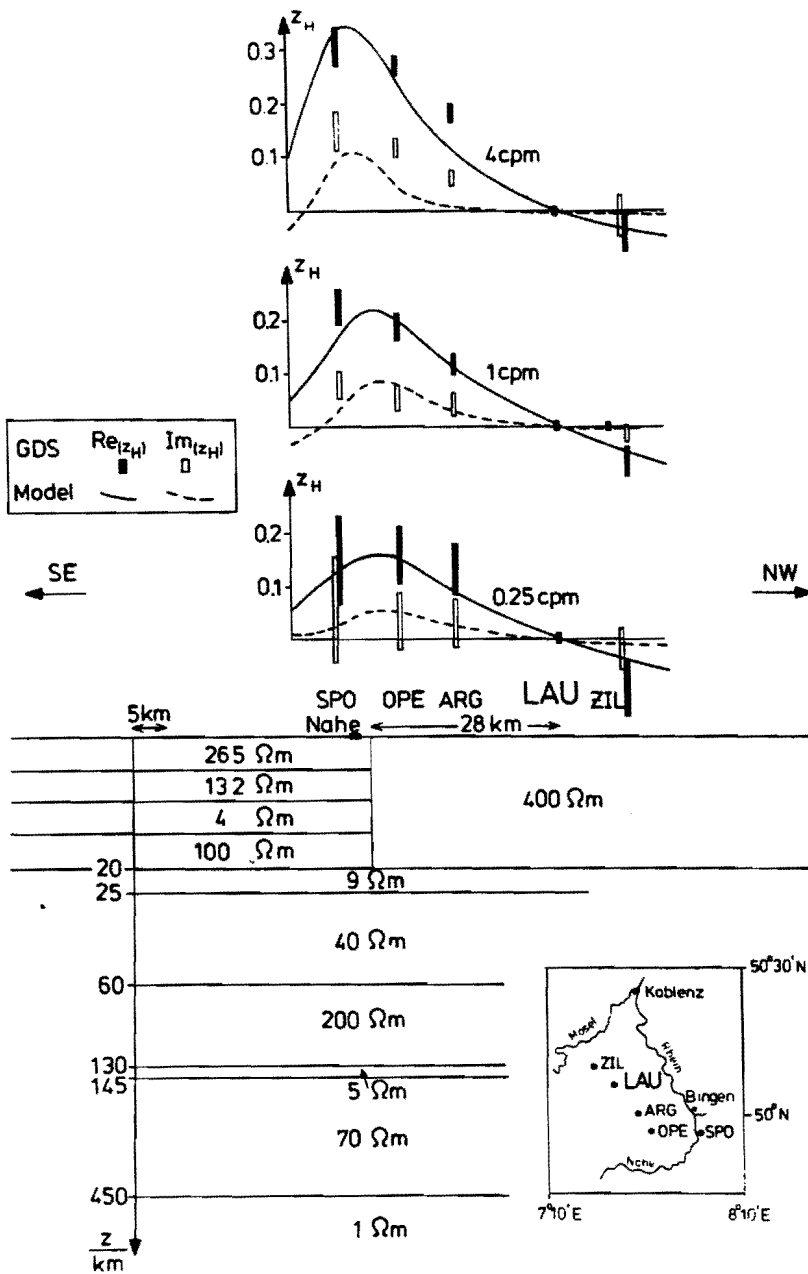
Fig. 2. Simplified 2D model of the resistivity distribution in a SE-NW-running vertical cut through the northern Rhinegraben and the Hunsrück. Site names SPO, OPE, etc. refer to z_H plots as well as to the conductivity cross-section. The *right block* and the laterally homogeneous layers from 20 km depth downwards show the vertical resistivity-depth profile of LAU as calculated from the impedance which is corrected for local distortions. The *left block* (up to 20 km depth) is derived from MT measurements at SPO. For further explanation, see text

3) Geomagnetic transfer functions z_H according to Eq. (3) on a depth sounding profile which connect both MT sites. z_H refers to the magnetic field in the x' direction.

Schmucker's (1971) 'inhomogeneous layer' algorithm is used for E- and B-polarization. The model is presented and explained in Fig.2. Adapting the impedance of the model to that measured at SPO works well over the whole period range. Figure 2 shows the adaption of the model-generated anomalous magnetic field transfer function z_H to the measured one. Figure 3 shows the adaption of both impedances measured at LAU. In addition to the two phases, the frequency dependence of the anisotropy Z'_{xy}/Z'_{yx} is also shown. The anisotropy remaining after splitting off a frequency-independent distortion matrix must be explained solely by use of the regional conductivity model. However, the unmodified anisotropy is also influenced by local distortion. The model incorporates a conducting layer at 20 km depth underneath the Hunsrück. This layer explains why the phase

of the E-polarization Z'_{yx} at LAU is 70° at frequencies around 100 cycles per hour (Fig. 3). It was also found by Jödicke et al. (1983). Field and model data show, correspondingly: (1) At 600 cph the phases are almost equal and the anisotropy corrected for local effects is near unity, i.e. a '1 D case'. (2) At longer periods the phase of the E-polarization Z'_{yx} exceeds that of the B-polarization z'_{xy} and the anisotropy becomes larger than 1. The conducting layer underneath the Hunsrück acts as a continuation of the low-resistive subsoil of SPO and decreases the phase of the B-polarization below 45° even though site LAU is on the highly resistive Rhenish Massif.

The distortion factors of the impedance at LAU were found for very long periods by independently adapting each impedance Z'_{xy}, Z'_{yx} to the undistorted impedance obtained from the $Z:H$ method (Bahr, 1985). The result was $a_{22} = 0.70$, $a_{11} = 1.75$ and a_{12} and a_{21} about zero in coordinates (x', y'). Therefore, the correction factor of the anisotropy

$|Z'_{xy}|/|Z'_{yx}|$

1.8
1.6
1.4
1.2
1.0
0.8

$|Z'_{xy}|/|Z'_{yx}|$
MT (corrected) +
Model x

75°

Φ

65°

55°

45°

35°

$\Phi(Z'_{yx})$ $\Phi(Z'_{xy})$
MT + +
Model x x

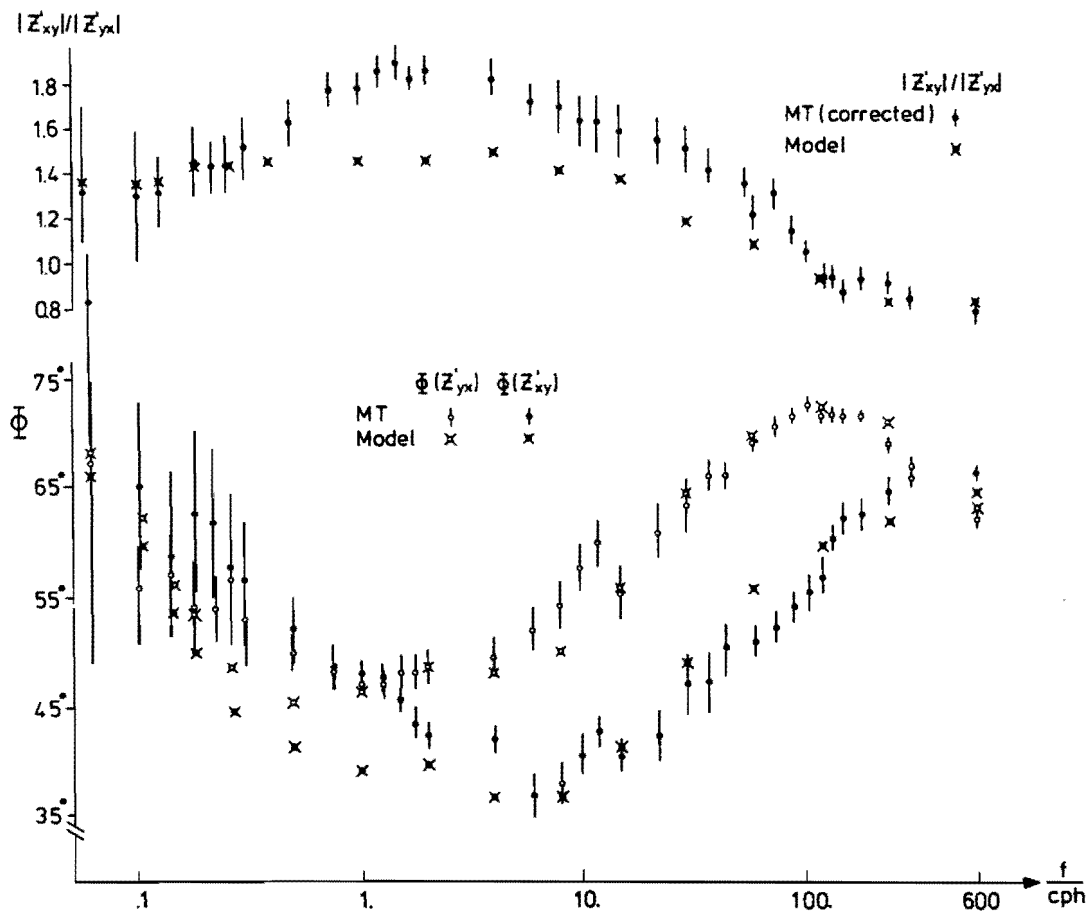.1   1.   10.   100.   600 $\frac{f}{cph}$

Fig. 3. Frequency dependence of the two phases and the impedance anisotropy of site LAU: measured values and those generated with the model described in Fig. 2. Z'_{yx} refers to E-polarization and Z'_{xy} refers to B-polarization

due to local distortion is $a_{11}/a_{22} = 2.50$. This factor is determined again here for all periods by comparing the model anisotropy describing the regional anomaly with the measured one.

The differences between measured and synthetic impedances at periods over 1 h probably arise from modelling the Rhenish Massif as an infinitely extended 2-D structure, although the penetration depth at these periods corresponds to its true extent. The phase of the synthetic impedances at longer periods changes if, instead of a 2-D model calculation, a 3-D one is used (Wannamaker et al., 1984).

The regional amplification of the vertical magnetic field is caused by the spatial change of conductance (Schmucker, 1970). Therefore, single-frequency data of the z_H transfer function are insufficient to detect a hidden shift of the impedance at site LAU because such a shift would vary the 'conductance jump' from LAU to SPO only slightly. However, the resolution of this reference conductivity method is enhanced when considering a wide frequency range. The depth of the conductive layer under the Rhenish Shield, which would also be biased by a hidden shift, can be determined by adapting the model to geomagnetic transfer functions at suitable frequencies. By use of this technique, Tezkan (1986) determines the depth of a conductive layer under the Black Forest where local distortions shift the impedance, hindering an accurate determination of this depth from MT data only.

Decoupling of local and regional anomalies

This section deals with the frequently occurring situation that the strike of the regional anomaly is initially unknown. With $Z_\perp$ and $Z_\parallel$ as the undistorted impedances of B- and E-polarization and $\mathbf{A}$ as the distortion matrix, the impedance tensor, in the coordinate system given by the strike of the regional anomaly, is:

$$\mathbf{Z} = \begin{pmatrix} a_{11} & a_{12} \\ a_{21} & a_{22} \end{pmatrix} \cdot \begin{pmatrix} 0 & Z_\perp \\ Z_\parallel & 0 \end{pmatrix} = \begin{pmatrix} a_{12}Z_\parallel & a_{11}Z_\perp \\ a_{22}Z_\parallel & a_{21}Z_\perp \end{pmatrix}. \tag{4}$$

$Z_\perp$ and $Z_\parallel$ are the inpedances of the regional 2-D anomaly. Each of them appears in one column of the impedance tensor. We consider 'telluric vectors'

$$\mathbf{e}'_x = a_{12}Z_\parallel \, \hat{x}' + a_{22}Z_\parallel \, \hat{y}'$$

and

$$\mathbf{e}'_y = a_{11}Z_\perp \, \hat{x}' + a_{21}Z_\perp \, \hat{y}', \tag{5}$$

where $\hat{x}'$ and $\hat{y}'$ are unit vectors. $\mathbf{e}'_x$ or $\mathbf{e}'_y$ defines an in-phase and an out-of-phase telluric vector with regard to the north or the east components of the magnetic field, respectively. If local anomalies are absent or if they are quasi 2-D in the same coordinates, $\mathbf{e}'_x$ points towards west and $\mathbf{e}'_y$ towards north. In the particular coordinate system which is consid-

ered here, the in-phase and the out-of-phase vector are parallel, but they are rotated out of their normal position:

$$a_{11} \neq 1, \quad a_{21} \neq 0, \quad a_{22} \neq 1, \quad a_{12} \neq 0.$$

In the (x, y) coordinates all elements of the impedance tensor contain different linear superpositions of $Z_\perp$ and $Z_\parallel$: the tensor is

$$\mathbf{Z} = \mathbf{T}^T \cdot \mathbf{A} \cdot \mathbf{Z}' \cdot \mathbf{T}, \tag{6}$$

where $\mathbf{T}$ is a rotation tensor and $\mathbf{A} \cdot \mathbf{Z}'$ is the impedance tensor described by Eq. (4). While in Eq. (4) only two phases occur, now each element of the impedance tensor has a different phase (compare Fig. 4). The expressions

$$S_1 = Z_{xx} + Z_{yy}, \quad S_2 = Z_{xy} + Z_{yx},$$
$$D_1 = Z_{xx} - Z_{yy}, \quad D_2 = Z_{xy} - Z_{yx} \tag{7}$$

are considered in the following instead of the original impedances. Transformation of these modified impedances into a new coordinate system which is rotated clockwise by an angle α yields

$$D_1' = D_1 \cos(2\alpha) + S_2 \sin(2\alpha)$$
$$S_2' = S_2 \cos(2\alpha) - D_1 \sin(2\alpha), \tag{8}$$

while S_1 and D_2 are rotationally invariant.

We wish to find the rotation angle α for which the transformed tensor takes the simple form of Eq. (4). The condition that the two elements Z_{xx} and Z_{yx} of the rotated impedance tensor which belong to the same telluric vector $\mathbf{e}_x$ have the same phase is $\mathrm{Im}(Z_{xx}/Z_{yx}) = 0$ or (Bahr, 1985)

$$\begin{aligned}
\frac{\mathrm{Re}(Z_{xx})}{\mathrm{Re}(Z_{yx})} &= \frac{\mathrm{Re}[S_1 + D_1 \cos(2\alpha) + S_2 \cdot \sin(2\alpha)]}{\mathrm{Re}[-D_2 - D_1 \sin(2\alpha) + S_2 \cdot \cos(2\alpha)]} \\
&= \frac{\mathrm{Im}[S_1 + D_1 \cos(2\alpha) + S_2 \cdot \sin(2\alpha)]}{\mathrm{Im}[-D_2 - D_1 \sin(2\alpha) + S_2 \cdot \cos(2\alpha)]} \\
&= \frac{\mathrm{Im}(Z_{xx})}{\mathrm{Im}(Z_{yx})}.
\end{aligned} \tag{9}$$

A similar condition exists which links the elements of the telluric vector $\mathbf{e}_y$.

The sine of the differences between the phases of each pair of impedances are now abbreviated by use of the 'commutators', e.g.

$$\begin{aligned}
[S_1, S_2] &= \mathrm{Re}(S_1) \, \mathrm{Im}(S_2) - \mathrm{Im}(S_1) \, \mathrm{Re}(S_2) \\
&= \mathrm{Im}(S_2 \cdot S_1^*) \tag{10}
\end{aligned}$$

($[D_1, D_2]$, $[D_1, S_2]$ and $[S_1, D_2]$ correspondingly).
Equation (9) with (10) becomes

$$-A \sin(2\alpha) + B \cos(2\alpha) + C = 0,$$

where

$$A = [S_1, D_1] + [S_2, D_2]$$
$$B = [S_1, S_2] - [D_1, D_2]$$
$$C = [D_1, S_2] - [S_1, D_2].$$

The solution is

$$\tan \alpha_{1,2} = \pm [(B+C)/(B-C) + (A/(B-C))^2]^{1/2} - A/(B-C). \tag{11}$$

The subscripts 1, 2, referring to the two different signs of the root in Eq. (11), describe two coordinate systems in which either the impedance tensor elements belonging to $\mathbf{e}_x'$ or those belonging to $\mathbf{e}_y'$ have the same phase.

If all elements of the impedance tensor have the same phase, it follows that $A = B = C = 0$ and no strike angle is obtained. Then the regional conductivity distribution is only depth dependent and $Z_\parallel = Z_\perp$ and Eq. (4) corresponds to Larsen's formulation, Eq. (1).

If the impedance tensor is exactly described by Eq. (4) in the appropriate coordinate system, it should be the case that $\alpha_1 = \alpha_2 - 90°$. Let

$$T_{90} = \begin{pmatrix} 0 & 1 \\ -1 & 0 \end{pmatrix}$$

be the tensor of a 90° rotation. Thus,

$$T_{90}^T \cdot \begin{pmatrix} a_{12} Z_\parallel & a_{11} Z_\perp \\ a_{22} Z_\parallel & a_{21} Z_\perp \end{pmatrix} \cdot T_{90} = \begin{pmatrix} a_{21} Z_\perp & -a_{22} Z_\parallel \\ -a_{11} Z_\perp & a_{12} Z_\parallel \end{pmatrix}. \tag{12}$$

At a rotation of 90°, the phases of $\mathbf{e}_x'$ and $\mathbf{e}_y'$ are commutable. The condition that the two angles which are due to the two different signs of the root in Eq. (11) differ by 90° leads to

$$\cot(\alpha_1 - \alpha_2) = 0$$

and therefore

$$C = [D_1, S_2] - [S_1, D_2] = 0. \tag{13}$$

The term C is rotationally invariant because S_1 and D_2 are so and

$$[D_1', S_2'] = [D_1, S_2]$$

as seen from Eqs. (8) and (10). C disappears, no matter which coordinate system is chosen, if the regional conductivity distribution is exactly two-dimensional. In a purely depth-dependent resistivity distribution, the condition

$$[D_1, S_2] = [S_1, D_2] = 0 \tag{14}$$

is fulfilled in addition.

A phase-sensitive skewness coefficient

The parameter C can be used to set up a new measure of the three-dimensionality of the regional conductivity distribution

$$\eta = \sqrt{C}/|D_2|. \tag{15}$$

It is related to the conventional skew

$$\kappa = |S_1|/|D_2| \tag{16}$$

by the ratio

$$\xi = \sqrt{C}/|S_1| = \eta/\kappa \tag{17}$$

of the phase-sensitive skew to the conventional skew. ξ^{-1} represents the relative contribution of local distortion to κ, e.g. for $\xi \ll 1$ it is totally determined by this distortion.
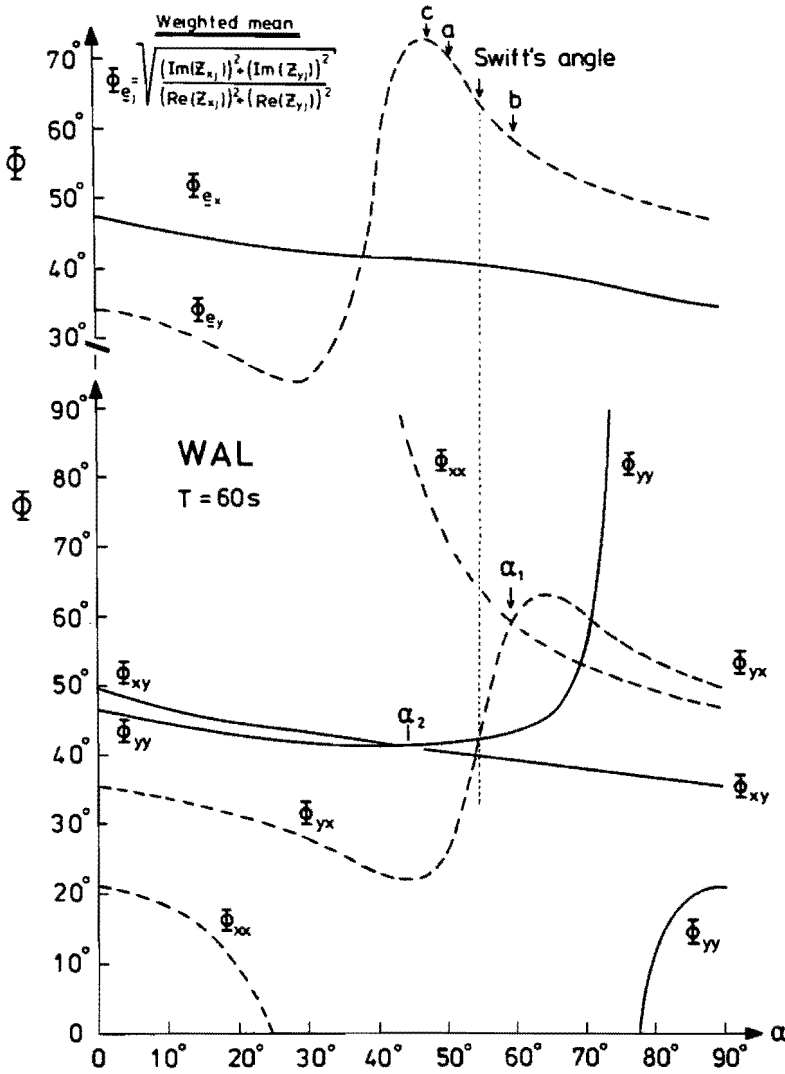
Fig. 4. Phases of the elements of the impedance tensor (*bottom*) and phases of the 'telluric vectors', according to Eq. (20), of site WAL, $T=1$ min, at a stepwise coordinate transformation. The impedances of the main diagonal elements are comparable with their confidence intervals for angles around 75° and 35°, and they have negative phases there. Then, it is not useful to calculate a phase according to Eq. (20) there. Elsewhere, $|\Delta Z/Z| < 0.1$ ($\beta = 68\%$) and $|\Delta \phi| < 5°$; the errors of all phases are smaller than the referred differences between ϕ_{e_x} and ϕ_{e_y}. For further explanation, see text

The strike of a regional 2-D anomaly

Swift's (1967) method to determine the strike of a 2-D structure leads to the analytical solution

$$\tan(4\alpha) = 2 \, \text{Re}(S_2 \cdot D_1)/(|D_1|^2 - |S_2|^2) \tag{18}$$

which depends on the moduli of the impedances, as does the skew [Eq. (16)]. Therefore, this formula may be inappropriate for finding the regional trend in the particular case where local telluric distortion determines those moduli.

A coordinate system in which one of the axes coincides with the strike of the regional anomaly and in which the impedance tensor takes the form of Eq. (4), can be found in various ways:

A) If $\eta < 0.1$, the regional anomaly is assumed to be exactly two-dimensional and C is set to zero:

$$\tan(2\alpha) = B/A. \tag{19}$$

To evaluate Eq. (11) or Eq. (19) the phases of all four elements of the impedance tensor have to be known. Random data errors can vary the value of η. If $\eta \neq 0$ due to data errors or deviations of the 2-D geometry, then $\alpha_1 - \alpha_2 \neq 90°$. This is demonstrated by use of field data from site WAL, a site within the Harz Mountains, representing

another uplifted and exposed piece of the Variscian mountain belt (Fig. 1). The phases of the four impedance tensor elements and their dependence on the chosen coordinate system are illustrated in Fig. 4. At $\alpha_2 = 47°$ the phases ϕ_{xy} and ϕ_{yy} which belong to e_y correspond, but the other two do not tally at all. At $\alpha_1 = 59°$ the phases belonging to e_x are exactly identical, the other two are almost identical. This behaviour leads to the second method.

B) The coordinate system defined by α_1, in which the phases of the 'rotation-sensitive' telluric vector e_x coincide, is used. That telluric vector is usually the one with the smaller moduli of impedance.

C) Changing from four to two phases can result in smoothing noisy data. Then, only the phases of the telluric vectors, defined by

$$\tan(\phi_{e_x}) = \left[\frac{(\text{Im } Z_{xx})^2 + (\text{Im } Z_{yx})^2}{(\text{Re } Z_{xx})^2 + (\text{Re } Z_{yx})^2}\right]^{1/2}$$

$$\tan(\phi_{e_y}) = \left[\frac{(\text{Im } Z_{xy})^2 + (\text{Im } Z_{yy})^2}{(\text{Re } Z_{xy})^2 + (\text{Re } Z_{yy})^2}\right]^{1/2} \tag{20}$$

are analysed. ϕ_{e_x} means the phase of the entire electric field correlated with the north component of the magnetic field,

with respect to that north component. As in the second method, the telluric vector whose phase is changed more profoundly by rotation, for example e_x, is searched for.

In the particular case where $[S_1, D_2] = 0$ and the skew κ is nevertheless non-zero, this skew can be explained by a maladjustment γ of the electrodes with respect to the magnetometer:

$$\frac{\mathrm{Re}(S_1)}{\mathrm{Re}(D_2)} = \frac{\mathrm{Im}(S_1)}{\mathrm{Im}(D_2)} = \tan(\gamma) \tag{21}$$

(Cox et al., 1980). This possibility cannot be distinguished from the case that in Eq. (4) one telluric vector dominates: $(a_{11}^2 + a_{21}^2)^{1/2} |Z_\perp| \gg (a_{12}^2 + a_{22}^2)^{1/2} |Z_\parallel|$. In that case, only $Z_\perp$ determines the phase of S_1 and D_2; and $\tan(\gamma) = a_{11}/a_{21}$ is the rotation of this telluric vector caused by local distortion.

Application to field data in the Harz Mountains

Table 1 shows both the modulus-sensitive and the phase-sensitive skew of three stations in the Harz Mountains. The NW-SE-striking southwest edge of the Harz, which delimits the Variscian sediments from the younger sediments of the Harz' southern forelands, can be considered as a regional 2-D anomaly with respect to two sites WAL, TEL (see Fig. 5). But the folding of the Variscian sediments is rotated by 70° from this direction: 'The Harz Mountains have an inner structure which runs southwest-northeast and a Hercynian stretched contour which runs northwest-southeast' (Mohr, 1978). Although the conventional skew [Eq. (16)] is large for stations WAL and TEL, the regional conductivity distribution is two-dimensional as indicated by the small phase-sensitive skew from Eq. (15). The folding acts like a 'local' anomaly and causes a linear polarization of the electric field in one preferred direction. Because this direction does not coincide with one of the axes of the coordinate system given by the regional 2-D anomaly, the conductivity distribution looks three-dimensional: $\kappa > \eta$.

At site PFE, a site on the Harzburg's gabbro massif, the situation is reversed. Here the regional conductivity distribution appears to be 3-D, but is concealed by a nearly 2-D local distortion, in which a_{11} is much larger than a_{22} but with a_{12} and a_{21} nearly zero in proper coordinates. The pronounced anisotropy a_{11}/a_{22} causes D_2 to overwhelm S_1. Therefore, the modulus-sensitive skew is small: $\kappa < \eta$.

The rotation angles for WAL, found with the help of Methods A), B), C), are marked in Fig. 4. Within the small angular interval $47° < \alpha < 59°$, one finds the phases $\phi_{e_y} = 40°$ and $\phi_{e_x} = 60°-70°$ according to Eq. (20). Swift's criterion Eq. (18) yields $\alpha = 55°$. But if only the off-diagonal elements are analysed in this coordinate system, one finds $\phi_{xy} \approx \phi_{yx} \approx 40°$. The phase bound to the telluric vector e_x is hidden by the distortion. The phases $\phi_{e_y} = 40°$ and $\phi_{e_x} = 65°$ at 1-min period correspond well to the two phases of site LAU (compare Fig. 3) and they can also be interpreted by a similar model of a high-resistive slab of a thickness limited to 20 km. Then, ϕ_{e_y} is the phase of the B-polarization with regard to the regional anomaly of the southwest edge of the Harz. But if both phases are taken to be about 40° according to Swift's criterion, there would be no clue to the lower boundary of the high-resistive domain.

Table 1. Skewness coefficients, according to Eqs. (15–17), of three sites at period $T = 1$ min

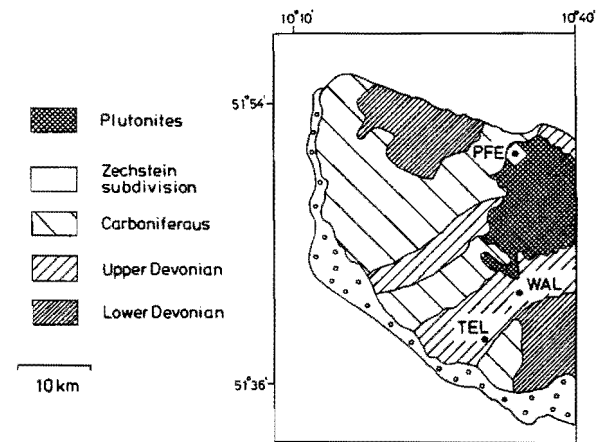| Station	κ	ζ	η
PFE	0.15	2.28	0.35
WAL	0.61	0.26	0.16
TEL	1.09	0.07	0.08

Fig. 5. MT stations in the Harz mountains

Comparison of methods

If only a regional 2-D structure but no top layer anomaly exists, the transformed impedances according to Eq. (7) reduce to

$$S_1' = 0 \qquad S_2' = Z_{xy}' + Z_{yx}'$$
$$D_1' = 0 \qquad D_2' = Z_{xy}' - Z_{yx}'$$

in a coordinate system given by the strike of the regional structure. If the coordinate system is rotated by an angle α, the impedances

$$S_1 = 0 \qquad\qquad S_2 = S_2' \cos(2\alpha)$$
$$D_1 = S_2' \sin(2\alpha) \qquad D_2 = D_2'$$

are observed. The conventional method of strike determination, Eq. (18), of course recovers the original strike. The phase-sensitive method yields

$$A = [S_2, D_2] \quad = [S_2', D_2'] \cos(2\alpha)$$
$$B = -[D_1, D_2] = -[S_2', D_2'] \sin(2\alpha)$$
$$C = [D_1, S_2] \quad = [S_2', S_2'] \sin(2\alpha) \cos(2\alpha) = 0$$

and

$$\tan(2\alpha) = B/A$$

from Eq. (19). Thus this method, too, recovers the original strike and yields a skew $\eta = 0$ according to Eq. (15).

In the opposite case, where only a surface anomaly exists, the conventional method [Eq. (18)] will still yield some strike direction. Gamble et al. (1982) suggest the determination of a regional strike from a generalization of Eq. (18). They replace the impedances D_1, S_2 by averages of those expressions obtained from several sites. This might result in a average of local strikes rather than a regional one.

Following Eggers (1982), those methods which try to give a complete representation of the impedance tensor are compared in the following, in terms of the number of degrees of freedom obtained:

1) The conventional coordinate transformation yields two principal impedances (4 degrees of freedom), the strike (1) and the skew (1). The ellipticity of the polarization ellipse S_1/D_2 provides additional information but not a full degree of freedom (Eggers, 1982). This method is 'incomplete' as it does not use all the information contained in the tensor.

2) Eggers' eigenstate formulation yields two complex eigenvalues (4), two non-orthogonal principal directions (2) and two ellipticities (2). This method gives a complete mathematical description of the MT tensor.

3) The method described in this paper deals with the impedances belonging to the two telluric vectors (4), the regional strike (1), the regional skew (1) and the distortion matrix (4). From the elements of the distortion matrix, the 'amplification' $(a_{12}^2 + a_{22}^2)^{1/2}$ and the angular deviation a_{12}/a_{22} of the telluric vector e_x as well as the equivalent distortion terms of e_y could be calculated. Ten independent parameters are necessary, while the impedance tensor provides only eight degrees of freedom. The additional two degrees of freedom are the static shifts of the impedances of the two telluric vectors: these amplifications, $(a_{12}^2 + a_{22}^2)^{1/2}$ and $(a_{11}^2 + a_{21}^2)^{1/2}$, remain unknown as long as no additional information besides the MT tensor is used.

The model of a regional 2-D conductivity structure and a superposed top layer anomaly has recently been treated by Zhang et al. (1987). They restrict their 'principal model' to a 2-D local structure. Therefore, the number of degrees of freedom due to local distortion is reduced by one; the four distortion matrix elements are replaced by a_{11}, a_{22} and the local strike. Assuming no regional skew, the principal model of Zhang et al. (1987) would have eight degrees of freedom, compared to ten degrees of freedom in the telluric-vector technique. Consequently, the authors offer a formula to calculate the two principal impedances without additional information besides the MT tensor. Any local structure should, however, have a limited extension. The model of a 2-D local structure, rather than a 3-D one, is a rough approximation which can be applied only in very few cases.

Haak (1972) suggested choosing a coordinate system for the electric field that minimizes the coherency between orthogonal electric components. The coordinate system of the magnetic field is rotated until the coherency between electric and magnetic fields reaches a maximum. An angular difference between the electric and magnetic coordinate systems indicates a 3-D conductivity distribution (Schwarz et al., 1984). This approach allows for non-orthogonal electric and magnetic fields, as does the telluric-vector technique. The latter, however, permits the two telluric vectors to have different deviations rather than associating one angular difference with the three-dimensionality of the strata.

Summary and conclusion

To choose an appropriate method of interpretation for a measured impedance tensor, one must ask whether all its elements have the same phase. If they do, it is sufficient to split the impedance tensor into a real distortion matrix and a scalar normal impedance. The distortion can be eliminated if either of these two quantities is known. They can both be determined by appropriate field measurements. If

the surface anomaly itself is of interest, the distortion matrix can be obtained from an examination of this surface anomaly by some DC method (Kemmerle, 1977). Where the conductivity of the mantle is to be investigated, the normal (undistorted) impedance can be calculated from magnetic long-period data with the $Z:H$ method (Larsen, 1977). The distortion matrix, which is obtained by comparing that normal impedance with the measured impedance tensor, can be applied to all shorter periods as long as only one phase appears in the tensor. Otherwise, the regional conductivity distribution is not purely depth dependent. By introducing a new, rotationally invariant skew, this paper suggests a test for the question of whether the regional structure is 2-D. It is the phases that are examined, not the amplitudes of the impedance tensor elements as in the conventional skewness analysis.

To explain the two phases of a seriously distorted impedance tensor of a site in the Rhenish Massif, a model calculation with a 2-D resistivity distribution which does not contain the local structures was carried out. Geomagnetic depth sounding data which are not influenced by the local structures were used as an additional check. As the model space includes a reference site with a known, undistorted impedance, there exists an initial value for the resistivity. By comparing the measured impedances with the modelled ones, real distortion coefficients were obtained. This 'reference conductivity' method offers another technique for removing DC distortion.

References

Bahr, K.: Joint interpretation of magnetotelluric and geomagnetic data and local telluric distortions. J. Geomagn. Geoelectr. **35**, 555–566, 1983

Bahr, K.: Magnetotellurische Messung des elektrischen Widerstandes der Erdkruste und des oberen Mantels in Gebieten mit lokalen und regionalen Leitfähigkeitsanomalien. Diss. Math.-Nat. Fachb. Univ. Göttingen, 1985

Cerv, V., Pek., J., Praus, O.: Models of geoelectrical anomalies in Czechoslovakia. J. Geophys. **55**, 161–168, 1984

Cevallos, C.: Magnetotelluric interpretation – another approach. PhD thesis, Macquarie University, Sidney, 1986

Counil, J.L., Le Mouël, J.L., Menvielle, M.: Associate and conjugate concepts in magnetotellurics. Ann. Géophys. **4**, B2, 115–130, 1986

Cox, C.S., Filloux, J.H., Gough, D.I., Larsen, J.C., Poehls, K.A., Herzen, R.P. von, Winter, R.: Atlantic lithosphere sounding. J. Geomagn. Geoelectr. **32**, Suppl. I, SI 13–32, 1980

Eckhardt, D.H.: Geomagnetic induction in a concentrically stratified earth. J. Geophys. Res. **68**, 6273–6278, 1983

Eggers, D.W.: An eigenstate formulation of the magnetotelluric impedance tensor. Geophysics **47**, 1204–1214, 1982

Gamble, T.D., Goubau, W.M., Miracky, R., Clarke, J.: Magnetotelluric regional strike. Geophysics **47**, 932–937, 1982

Haak, V.: Bestimmung der Übertragungsfunktionen in Gebieten mit lateraler Änderung der elektrischen Leitfähigkeit. Z. Geophys. **38**, 85–102, 1972

Jödicke, H., Untiedt, J., Olgemann, W., Schulte, L., Wagenitz, V.: Electrical conductivity structure of the crust and upper mantle beneath the Rhenish Massif. In: Plateau uplift, K. Fuchs, ed. Berlin, Heidelberg, New York, Tokyo: Springer 1983

Kemmerle, K.: Magnetotellurik am Alpen-Nordrand mit Diskus-

sion der lokalen Effekte und Darstellung einer Einzeleffekt-Auswertung. Diss. Fachb. Geowissenschaften, München, 1977

Larsen, J.C.: Removal of local surface conductivity effects from low frequency mantle response curves. Acta Geodaet., Geophys. et Montanist. Acad. Sci. Hung. 12, 183–186, 1977

LaTorraca, G.A., Madden, T.R., Korringa, J.: An analysis of the magnetotelluric impedance tensor for three-dimensional structures. Geophysics 51, 1819–1829, 1986

Mohr, K.: Geologie und Minerallagerstätten des Harzes. Stuttgart: Schweizerbart 1978

Schmucker, U.: Anomalies of geomagnetic variations in the southwestern United States. Bull. Scripps. Inst. Ocean., Univ. Calif., 13, 1970

Schmucker, U.: Neue Rechenmethoden zur Tiefensondierung. In: Protokoll Kolloquium Erdmagnetische Tiefensondierung, Rothenberge/Westfalen, P. Weidelt, ed.: 1–31, Geophysical Institute, Univ. Göttingen, 1971

Schmucker, U.: Erdmagnetische Tiefensondierung mit langperiodischen Variationen. In: Protokoll Kolloquium Erdmagnetische Tiefensondierung, Grafrath/Bayern, A. Berktold, ed.: 313–342, Geophysical Institute, Univ. München, 1974

Schwarz, G., Haak, V., Martinez, E., Bannister, J.: The electrical conductivity of the Andean crust in northern Chile and southern Bolivia as inferred from magnetotelluric measurements. J. Geophys. 55, 169–178, 1984

Swift, C.M.: A magnetotelluric investigation of an electrical conductivity anomaly in the southwestern United States. Ph.D. thesis, M.I.T., Cambridge, Mass., 1967

Tezkan, B.: Erdmagnetische und magnetotellurische Untersuchungen auf den hochohmigen Kristallinstrukturen des Hochschwarzwaldes und des Bayerischen Waldes bei Passau. Diss. Math.-Nat. Fachb. Univ. Göttingen, 1986

Wannamaker, P.E., Hohmann, G.W., Ward, S.H.: Magnetotelluric responses of three-dimensional bodies in layered earths. Geophysics 49, 1517–1533, 1984

Yee, E., Paulson, K.V.: The canonical decomposition and its relationship to other forms of magnetotelluric impedance tensor analysis. J. Geophys 61, 173–189, 1987

Zhang, P., Roberts, R.G., Pedersen, L.B.: Magnetotelluric strike rules. Geophysics 52, 267–278, 1987